Khattak et al., *Cogent Engineering* (2015), 2: 1050324
http://dx.doi.org/10.1080/23311916.2015.1050324

cogent engineering

MATERIALS ENGINEERING | RESEARCH ARTICLE

Magnetocaloric properties of metallic nanostructures

Khurram S. Khattak[1], Amir Aslani[1]*, Chidubem A. Nwokoye[1], Abid Siddique[1], Lawrence H. Bennett[1] and Edward Della Torre[1]

Received: 13 March 2015
Accepted: 05 May 2015
Published: 29 June 2015

*Corresponding author: Amir Aslani, Department of Electrical and Computer Engineering, Institute for Magnetics Research, The George Washington University, Washington, DC 20052, USA
E-mail: aaslani@gwu.edu

Reviewing editor:
Eileen Harkin-Jones, Queen's University Belfast, UK

Additional information is available at the end of the article

Abstract: A compilation of magnetocaloric properties of metallic nanostructures with Curie temperature (T_C) between 260 and 340 K has been tabulated. The tabulated data show that nanostructure plays an important role in enhancing the magnetocaloric properties of a material, namely by reducing the peak of magnetic entropy, but broadening of the magnetocaloric effect curve with an average of 10 K sliding window for Curie temperature. A second table lists all bulk metallic and intermetallic materials, in which there is no nanostructural data, with an entropy change of at least 20 J/kg K and a Curie temperature between 260 and 340 K. We propose that further experiments should be made on the nanostructured form of these materials.

Subjects: Electrical & Electronic Engineering; Materials Science; Nanoscience & Nanotechnology

Keywords: nanostructure; magnetocaloric effect; magnetic refrigeration; Curie temperature; entropy change; relative cooling power

1. Introduction

Magnetic refrigeration technology, as a promising alternative to conventional gas compression cooling, has attracted extensive attention due to its good energy efficiency, and environmentally friendly

ABOUT THE AUTHORS

Authors are focusing their cutting-edge research at the Institute for Magnetics Research (IMR) of the George Washington University on modeling, experimental measurements, and the use of magnetic materials. The materials most commonly studied are magnetic recording media, magneto-optical media, magnetocaloric material, and magnetostrictive material. Some of the applications for such materials include computer hard drives, memories, microwave devices, magnetostrictive transducers, and magnetic refrigeration. Modeling methods employed include Preisach-based models, micromagnetics, and nonlinear finite element models. IMR has several well-equipped laboratories such as Magnetic Refrigeration Research Laboratory, Magnetic Material Testing Laboratory, and Magneto-Optics Laboratory. Past and present organizations that have cooperated with the Institute in conducting research include NIST, NSF, DOE, ONR, GE Global Research, BEP, DARPA, IBM, Fuji, and ANSYS Software.

PUBLIC INTEREST STATEMENT

In contrast with conventional refrigerator systems that work based on compression and evaporation of gas, magnetic refrigeration systems work based on magnetizing and demagnetizing a magnetic material. Magnetic refrigeration is an energy-efficient and environmentally friendly refrigeration technology with the following desirable characteristics: (1) it does not use ozone-depleting and hazardous chemicals or greenhouse gases; (2) the cooling efficiency of magnetic refrigeration is significantly higher than conventional cooling technology, compressor-based techniques; and (3) the magnetic refrigerator can be built more compactly and generates less noise. Magnetic refrigeration exploits a property of magnetic materials called the magnetocaloric effect (MCE). A through literature survey has been done in this article and it has been concluded that metallic nanostructures are the best materials to be used in a magnetic refrigeration system compared to their bulk counterparts. Moreover, this paper suggests some new materials to be synthesized as nanostructures and their MCE properties studied.

nature. Materials with Curie temperature near room temperature with good magnetocaloric effect (MCE) properties and negligible hysteresis are of special interest.

Particle size, shape, morphology, chemical composition, structure, and interaction of the particle with the surrounding matrix and neighboring particles all have a profound effect on the magnetic behavior of the material. Any material with discrete functional parts, with any internal, external, or surface structure dimension of the order of 100 nm or less is classified as nanostructured material. Nanostructures can be synthesized in different shapes such as nanowires, nanotubes, etc. Differentiation between the numbers of dimensions on the nanoscale describes a nanostructured material. It has been shown that nanostructures are the best choice for magnetic refrigeration systems (Bennett et al., 1995; Della Torre, Bennett, & Jin, 2012; Shir, Yanik, Bennett, Della Torre, & Shull, 2003; Shull, Swartzendruber, & Bennett, 1991). Nanostructures have a higher MCE over a temperature distribution so they exhibit more cooling efficiency as compared to bulk materials. The entropy change ΔS, determines the cooling efficiency and it is largest at lower fields. The magnitude of entropy change varies for different materials based on the number of particles per unit volume, magnetic moment of the particles, and the order parameter (Shir et al., 2003). An example of this can be seen in Figures 1 and 2 for gadolinium. Magnetocaloric properties of a nanostructure can be tuned and optimized by controlling its properties such as size, shape, morphology, etc. Therefore, the MCE peak can be displaced to other temperatures, broadened, or made sharper. This point has been amplified, by gathering all nanostructures with Curie temperature in the range of 260–340 K in Table 1 and comparing their MCE properties to their bulk counterparts for materials available in the literature. Furthermore, all bulk materials reported in the literature with magnetic entropy of at least 20 J/kg K and a Curie temperature between 260 and 340 K have been arranged in Table 2. This list is of importance for future research since there are no data available for the nanostructurized form of these bulk materials.

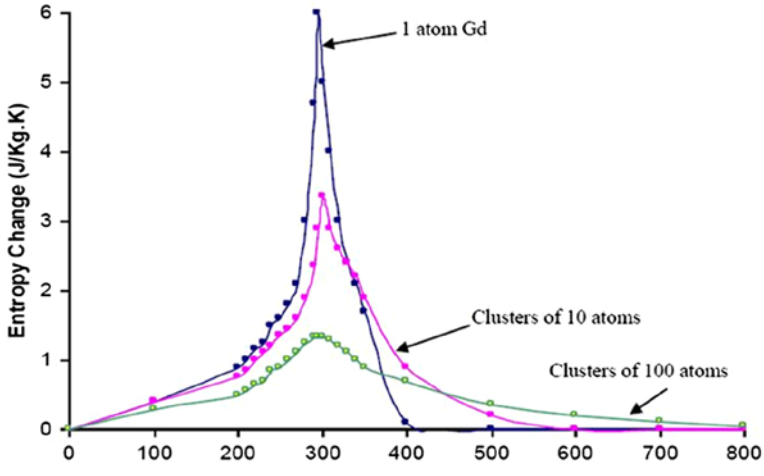

Figure 1. Calculated change in entropy, $|\Delta S_m|$, of nanocomposite clusters of Gd and Gd alloys between 0 and 2*T* vs. temperature.

Notes: The one atom calculation agrees with the bulk Gd experimental results. The alloys must be chosen so as to keep the ordering temperature the same as that of bulk Gd (Shir et al., 2003).

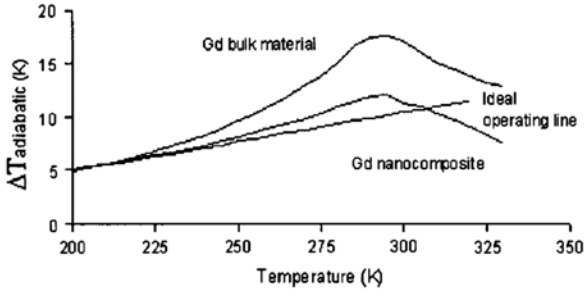

Figure 2. MCE (ΔT) vs. temperature for the operating lines: ideal Gd bulk material and a calculated Gd nanocomposite (Shir et al., 2003).

Table 1. Studied nanostructured materials and their bulk counterparts

Sample	Size (nm)	T_C (K)	$\Delta\lvert S_M\rvert$ (J/kg K)	ΔT_{ad} (K)	ΔH (kOe)	RCP (J/kg)	Reference
Pr_2Fe_{17}	20	292	4.5		50	573	Gorria et al. (2008)
	B	286	6.4		50	506	Gorria et al. (2008)
	20	292	2.1		15	107	Alvarez, Sánchez-Marcos, et al. (2010)
	B	285	2.6		15	105	Alvarez, Sánchez-Marcos, et al. (2010)
Nd_2Fe_{17}	14	340	1.6		15	83	Alvarez, Gorria, et al. (2010)
	24	340	1.85		15	87	Alvarez, Gorria, et al. (2010)
	B	339	2.6		15	87	Alvarez, Gorria, et al. (2010)
	17	340	1.2		15	87	Alvarez, Sánchez-Marcos, et al. (2010)
	B	339	1.7		15	82	Alvarez, Sánchez-Marcos, et al. (2010)
$NdPrFe_{17}$	20	303	2.1		20	175	Sánchez-Valdés et al. (2014)
$Fe_{72}Ni_{28}$		333	0.5		50	250	Ucar et al. (2013)
$Fe_{70}Ni_{30}$		333	0.32		50	342	Ucar et al. (2013)
$(Fe_{70}Ni_{30})_{97}Mo_3$		320	1.69		50	440	Ucar et al. (2014)
$(Fe_{70}Ni_{30})_{96}Mo_3$		300	1.67		50	432	Ucar et al. (2014)
$Co:Ni_{67}Cu_{33}$	2	260	0.15		10	18*	Michalski et al. (2012)
		270	0.72		70	108*	Michalski et al. (2012)
Co/Cr superlattices		334	0.27*	0.3	50		Mukherjee et al. (2009)
$Fe_x Pt_{100-x}$							Rong et al. (2007)
$CuCr_2Te_4$	22	330					Ramasamy et al. (2012)
$MnAs_{0.97}P_{0.03}$	23	275	14		50	294*	Sun et al. (2012)
Gd	15	288		1.1			Zeng, Kuang, Zhang, and Yue (2012)
	100	296		2.1			Zeng et al. (2012)

Notes: Size (nm), Curie temperature (K), magnetic entropy change (J/kg K), adiabatic temperature (K), magnetic field (kOe), and RCP_{FWHM} (J/kg). B refers to bulk.
*Own calculation from the figures.

Though much research has been done on employing oxide nanostructures, oxide nanostructures have less magnetization and will not be able to compete with metallic nanostructures. Therefore, metallic and intermetallic nanostructures seem to be the best choice for magnetic refrigeration systems.

2. Methodology

Nanostructures have several advantages as a refrigerant for 100–300-K applications compared to the other common methods of assembling a magnetic refrigeration bed, such as a layered thermal bed (Shir et al., 2003) or mixing of different magnetic materials. In order to predict and evaluate the MCE of a nanostructure, refrigerant capacity can be considered as the basis for calculating the temperature behavior of the material. The relative cooling power (RCP) is defined as

$$\mathrm{RCP} = -\Delta S_M(T, H) \times \delta T_{\mathrm{FWHM}}, \tag{1}$$

where $\Delta S_M(T, H)$ is the refrigerant's magnetic entropy change as a function of temperature and magnetic field and δT_{FWHM} is the full width at half maximum (FWHM) of the peak of magnetic entropy. This parameter measures how much heat can be transferred between the cold and hot heat exchangers in an ideal refrigeration cycle (Gschneidner, Pecharsky, Pecharsky, & Zimm, 1999; McMichael, Shull, Swartzendruber, Bennett, & Watson, 1992). Increasing the RCP not only increases the amount of refrigeration obtainable from the particular refrigerant and field excursion, but also tends to increase the thermodynamic efficiency of the cycle, thus measuring how well a particular volume or quantity of refrigerant is utilized. Improvement in RCP mainly relies on broadening the magnetic entropy change by either coupling two phases of magnetic materials with desirable properties or nanostructure synthesis with the main

Table 2. Metallic and intermetallic bulk materials with magnetic entropy of at least 20 J/kg K

Sample	T_C (K)	$\Delta\|S_M\|$ (J/kg K)	ΔT_{ad} (K)	ΔH (kOe)	RCP (J/kg)	Reference
$LaFe_{11.2}Co_{0.7}Si_{1.1}$	274	20.3		50	670*	Hu, Shen, Sun, Wang, and Cheng (2002)
$La(Fe_{0.94}Co_{0.06})_{11.9}Si_{1.1}$	274	20**	2.5	50	400*	Hu et al. (2005)
$LaFe_{11.7}Si_{1.3}Co_{0.2}H_{1.7}$	278	23.9		50	956*	Zhang et al. (2012, 2013)
$La(Fe_{0.89}Si_{0.11)13}H_{1.4}$	298	24**		20	192*	Fujieda, Fujita, Fukamichi, and Suzuki (2011)
$La_{0.5}Pr_{0.5}Fe_{11.4}Si_{1.6}H_{0.9}$	275	24.1		50	366	Zhao et al. (2010)
$La_{0.5}Pr_{0.5}Fe_{11.4}Si_{1.6}H_{1.6}$	317	22.1		50	351	Zhao et al. (2010)
$La(Fe_{0.88}Si_{0.12})_{13}H_{1.5}$	325**	24	12.6	50		Fujieda, Fujita, and Fukamichi (2007)
$La_{0.5}Pr_{0.5}(Fe_{0.88}Si_{0.12})_{13}H_{1.6}$	320**	26	13.6	50		Fujieda et al. (2007)
$La(Fe_{0.88}Si_{0.12)13}H$	274	23	11.1	50	460*	Fujita, Fujieda, Hasegawa, and Fukamichi (2003)
$La(Fe_{0.88}Si_{0.12)13}H_{1.5}$	323	23	12.6	50	506*	Fujieda et al. (2003)
$La(Fe_{0.89}Si_{0.11)13}H_{1.3}$	291	28	12.8	50	–	Fujieda et al. (2003)
$La(Fe_{0.9}Si_{0.1)13}H_{1.1}$	287	31	15.4	50	–	Fujieda et al. (2003)
$Gd_5Si_{1.95-x}Ge_{2.04}Sn_{0.01}$	270	22**		20	132*	Li et al. (2006)
$Gd_5Si_{1.95-x}Ge_{2.02}Sn_{0.03}$	277	28.9		20	87*	Li et al. (2006)
$Gd_5Si_{1.95-x}Ge_2Sn_{0.05}$	268	25**		20	188*	Li et al. (2006)
$Gd_5Si_{1.95-x}Ge_{1.95}Sn_{0.1}$	260	23**		20	69*	Li et al. (2006)
$Mn_{0.9}Cr_{0.1}As$	267	20.2		50	283*	Sun et al. (2008)
MnAs	318**	38**		50	418*	Balli et al. (2008)
$Mn_{0.9}Ti_{0.05}V_{0.05}As$	266**	31**		50	256*	Balli et al. (2008)
$MnAs_{0.927}Sb_{0.073}$	305**	27.5**		10	55*	Kim, Wada, and Itoh (2007)
MnAs	316	28.8–40		20–50	267	Tocado, Palacios, and Burriel (2006, 2009), Gama et al. (2004), Mosca, Vidal, and Etgens (2008)
$Mn_{0.99}Fe_{0.01}As$	294	26		20		Balli, Fruchart, Gignoux, and Zach (2009)
$Mn_{0.9875}Cr_{0.0125}As$	300**	38	15**	50	893	Mejia, Gomes, Reis, and Rocco (2011)
$Mn_{0.9875}Cr_{0.0065}Fe_{x0.006}As$	287**	42	13.5**	50	730	Mejia et al. (2011)
$Mn_{0.94}Fe_{0.06}As$	289	29.3		50		Lima Sharma, Gama, Coelho, and de Campos (2008)
$Mn_{0.94}Cu_{0.06}As$	308	21		50		Lima Sharma et al. (2008)
$MnAs_{0.93}Sb_{0.07}$	273**	30**		29	260*	Wada, Matsuo, and Mitsuda (2009)
$MnAs_{0.99}P_{0.01}$	301**	40	13	140	–	Mitsiuk, Govor, and Budzynski (2013)
$MnAs_{0.98}P_{0.02}$	296**	50	15	140	400*	Mitsiuk et al. (2013)
$Mn_{0.985}Fe_{0.015}As$	280**	30**		80	300*	Bratko et al. (2012)
$MnFeP_{0.5}As_{078}Ge_{0.22}$	280	38**		50	760*	Dagula et al. (2005)
$MnFeP_{0.5}As_{077}Ge_{0.23}$	309**	31**		50	465*	Dagula et al. (2005)
$MnFeP_{0.5}As_{0.4}Si_{0.1}$	303	20		30	240*	Dagula et al. (2006)
$MnFeP_{0.5}As_{0.3}Si_{0.2}$	294	32		30	192*	Dagula et al. (2006)
$MnFeP_{0.5}As_{0.2}Si_{0.3}$	280	21		30	210*	Dagula et al. (2006)
$Mn_{1.1}Fe_{0.9}P_{0.76}Ge_{0.24}$ (Ribbon)	317	35.4		50	496*	Yan, Müller, Schultz, and Gutfleisch (2006)
$Mn_{1.1}Fe_{0.9}P_{0.76}Ge_{0.24}$ (Bulk)	299	26.1		50	522*	Yan et al. (2006)
$MnFe_{0.9}P_{0.78}Ge_{0.22}$	296	20		20	200*	Trung et al. (2009)
$Mn_{1.2}Fe_{0.8}P_{0.75}Ge_{0.25}$	288	20.3		20	151	Trung et al. (2009)
$Mn_{1.1}Fe_{0.9}P_{0.5}As_{0.5}$	274**	21		40	300	Gribanov et al. (2009)
$Mn_{1.1}Fe_{0.9}P_{0.8}Ge_{0.2}$	267.5	44.35		30	311*	Yue et al. (2010)
$Mn_{x1.20}Fe_{0.75}P_{0.50}Si_{0.50}$	299**	26**		20	260*	Dung, Zhang, Ou, Brück, and Zhang (2011)

(*Continued*)

Table 2. (*Continued*)

Sample	T_C (K)	$\Delta\|S_M\|$ (J/kg K)	ΔT_{ad} (K)	ΔH (kOe)	RCP (J/kg)	Reference
$Mn_{x1.25}Fe_{0.7}P_{0.50}Si_{0.50}$	285**	22**		20	176*	Dung et al. (2011)
$Mn_{1.1}Fe_{0.9}P_{0.76}Ge_{0.24}$	280**	46.5		50	558*	Yue et al. (2013)
$Mn_{1.1}Fe_{0.9}P_{0.78}Ge_{0.22}$	298	20	4	20	160*	Sougrati et al. (2008)
$Mn_{0.92}Cu_{0.08}CoGe$	321	53.3		50	267*	Samanta, Dubenko, Quetz, Stadler, and Ali (2012)
$Mn_{0.915}Cu_{0.085}CoGe$	304	52.5		50	210*	Samanta et al. (2012)
$Mn_{0.91}Cu_{0.09}CoGe$	289	41.2		50	124*	Samanta et al. (2012)
$Mn_{0.905}Cu_{0.095}CoGe$	275	34.8		50	314*	Samanta et al. (2012)
$MnCo_{0.55}Zn_{0.45}Ge$	327	26		50	286*	Samanta, Dubenko, Quetz, Stadler, and Ali (2013)
$MnCo_{0.95}Zn_{0.05}Ge$	281	31.4		50	252*	Samanta et al. (2013)
$Mn_{0.93}Cr_{0.07}CoGe$	265**	23**		50	230*	Caron, Trung, and Brück (2011)
$Mn_{2.6}Fe_{0.4}Sn_2$	260	24.6		50	1,380	Recour, Mazet, and Malaman (2008)
$Mn_{2.5}Fe_{0.5}Sn_2$	261	23.9		50	1,390	Recour et al. (2008)
$Mn_{2.4}Fe_{0.6}Sn_2$	268	25.3		50	1,570	Recour et al. (2008)
$Mn_{2.3}Fe_{0.7}Sn_2$	271	24.4		50	1,510	Recour et al. (2008)
$Mn_{2.2}Fe_{0.8}Sn_2$	283	23		50	1,380	Recour et al. (2008)
$Mn_{2.1}Fe_{0.9}Sn_2$	290	20.6		50	1,350	Recour et al. (2008)
Gd_7Pd_3	328**	56.8	8.5	50	373	Canepa, Cirafici, Napoletano, and Merlo (2002)
Gd_7Pd_3Ni	315**	41.1	6.8	50	240	Canepa et al. (2002)
$Gd_{76}Pd_{24}$	300**	56.1	8.4	50	422	Canepa et al. (2002)
$Fe_{80}Pt_{20}$	283**	25.2		50	530*	Rongm and Ping Liu (2007)

Notes: Curie temperature (K), magnetic entropy change (J/kg K), adiabatic temperature (K), magnetic field (kOe), and RCP (J/kg).

*Own calculation from the figures.

**Approximation from the figures in the references.

motivation rooted in their inherent tendency to have distributed exchange coupling, which will broaden the magnetic entropy curve (Ucar, Ipus, France, Mchenry, & Laughlin, 2012).

The sum rule (McMichael et al., 1992) implies that for materials with the same saturation magnetic moments, M_o, those with high entropy change at a given temperature will have low entropy changes at other temperatures, and materials which do not have a large entropy change at any particular temperature can undergo a moderate entropy change over a broader temperature range. Magnetization of suitable nanostructures can be switched by an applied magnetic field of the order 1 T (10 kOe) or less, which is easily realized without using superconducting magnet (Skomski, Binek, Mukherjee, Sahoo, & Sellmyer, 2008).

The need for obtaining materials with a desired entropy change leads to the need for accurate modeling and simulation of entropy change for materials. Work by Bennett, McMichael, Tang, and Watson (Bennett, McMichael, Tang, & Watson, 1994) and Bennett, McMichael, Swartzendruber, and Shull (Bennett, McMichael, Swartzendruber, & Shull, 1992) shows how Monte Carlo simulations can be used to predict entropy change for a nanostructure with ferromagnetically interacting clusters. Results in McMichael et al. (1992) and Bennett et al. (1992) show that magnetic nanostructures can possess enhanced magnetocaloric properties at high temperatures and low fields. Materials that rely on nanostructures include paramagnetic salts used for attaining low temperatures and superparamagnetic particles for intermediate temperatures, while on ferromagnetic to paramagnetic or magnetostructural phase transformation at room temperature (Ucar et al., 2012).

Work by Shir et al. (2003) emphasizes that magnetic nanostructures with interacting clusters are a means by which to readjust magnetic entropy (Δ*S*) to make it more uniform with the temperature and to provide enhanced magnetic entropy (Δ*S*) values at temperatures above their effective interaction temperature. In addition, they revealed that by appropriate selection of nanostructure materials, MCE vs. *T* curve can be fine-tuned to a specific curve as shown in Figures 1 and 2. Magnetic entropy (Δ*S*) constancy can be fulfilled and in the reversible case, the cycle will have an efficiency equivalent to the Carnot cycle.

Work by Shull (Shull, 1993) shows experimental and theoretical verifications of the enhancement of magnetocaloric properties of a superparamagnetic nanostructure material $Gd_3Ga_{5-x}Fe_xO_{12}$ (GGIG) at high temperatures and low fields. In addition, the MCEs were found to be 3–4 times larger than a low temperature paramagnetic refrigerant (GGG).

Nanostructuring improves the entropy change in low fields and high temperatures, but yields some reduction in the maximum entropy change per atom. An important feature of magnetic nanoparticles is that the entropy exhibits a strong dependence on the magnetic anisotropy which can be exploited for magnetic cooling (Skomski et al., 2008). In principle, anisotropy of nanostructures can be tailored almost at will, being possible to control not only its magnitude but also the distribution of easy axes orientation, leading to MCE response that is qualitatively different to that of the bulk material (Franco et al., 2008). Inter-particle and intra-particle interactions modify the magnetic responses for an arrangement of nanoparticles such as anisotropy energy (Skomski et al., 2008), Zeeman energy, and dipolar interaction energy. The total energy is given by

$$E = \sum_i E_A^{(i)} + \sum_i E_H^{(i)} + \frac{1}{2}\sum_i \sum_{j \neq i} E_D^{(i,j)}, \tag{2}$$

in which, the anisotropy and Zeeman energy terms are $E_A^{(i)} = -kV_i\left((\mu_i \cdot n_i)/|\mu_i|\right)^2$ and $E_H^{(i)} = -\mu_i \cdot H$, respectively. The magnetic dipole energy between two particles *i* and *j*, separated by a distance r_{ij}, with magnetic moments μ_i and μ_j, and the volume corresponding to the *i*th particle V_i, is $E_D^{(i,j)} = \frac{\mu_i \cdot \mu_j}{r_{ij}^3} - \frac{3(\mu_i \cdot r_{ij})(\mu_i \cdot r_{ij})}{r_{ij}^5}$.

Inter-particle interactions' strength exhibits three magnetic stages: (1) Superparamagnetism (SPM) for no interaction, (2) Superspin glass (SSG) for intermediate interaction strengths, and (3) Superferromagnetism for highly interacting superspins (Bedanta & Kleemann, 2009). Detailed studies on the effect of different parameters e.g. particle size, inter-particle distance, magnetic field, and temperature on the above states are discussed in Chen, Sahoo, Kleemann, Cardoso, and Freitas (Chen, Sahoo, Kleemann, Cardoso, & Freitas, 2004) and Petracic et al. (Petracic et al., 2006).

3. Sample preparation

Properties of materials, in general, and nanoparticles, in particular, are influenced by shape, size, and other parameters controlled by sample preparation. Hence, a special interest in the field of sample preparation. Broadly techniques can be classified into top-down or bottom-up approaches as shown in Figure 3.

Many current strategies combine both synthesis and assembly into a single process (Gubin, Koksharov, Khomutov, & Yurkov, 2005; Saravanan, Gopalan, & Chandrasekaran, 2008). Some of these techniques are

- High-temperature Thermal Decomposition which is suitable for preparing films of nanoparticles (Saravanan et al., 2008).
- Gas–liquid Interface for the synthesis of metallic nanoparticles in the absence of solid substrates or matrices by oxidation–reduction (redox) reactions at an interface between two phases, one containing a metal compound and the other, the reducing agent (Saravanan et al., 2008).

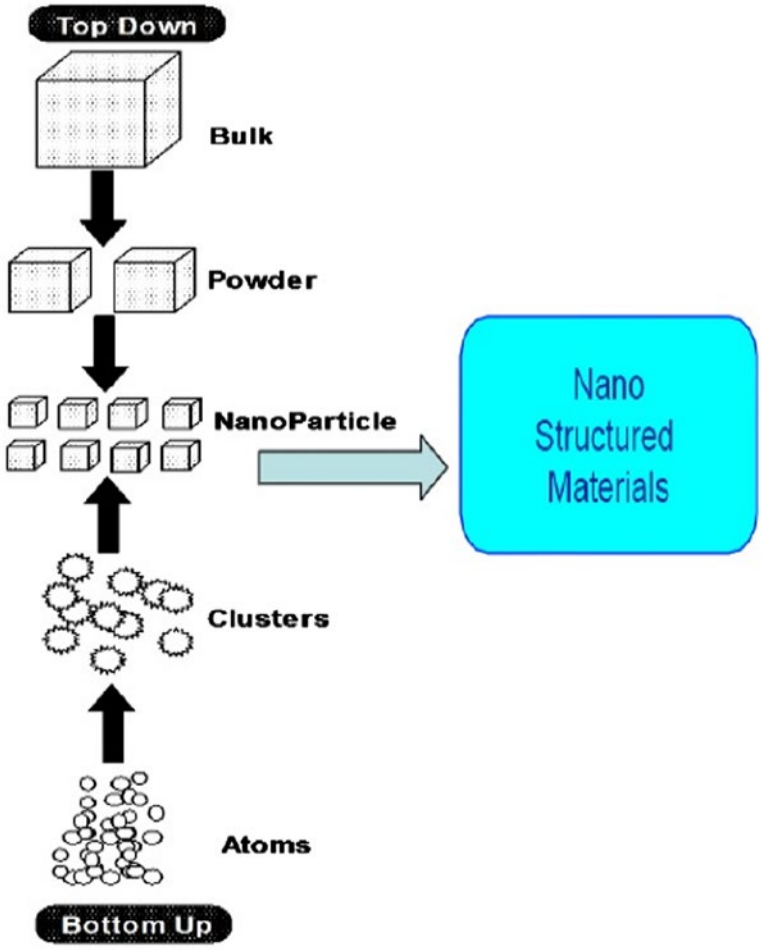

Figure 3. Nanostructure fabrication processes.

- Electrolytic erosion and electrochemical generation are examples of Mechanochemical dispersion, which is an attractive way to produce disperse systems with the size of the particles depending upon the density of the electric current (Saravanan et al., 2008).
- Liquid–liquid Interface Reaction not only synthesizes nanoparticles but also casts them into a film in one process (Gubin et al., 2005).
- Vaporization (laser, thermal, plasma, arch discharge, and solar energy-induced) of supersaturated metal allows to study physiochemical characteristics and properties at the gas and solidified phases (Gubin et al., 2005).
- Thermolysis or Thermal decomposition of metal-containing compounds is carried out in a liquid medium in the presence of surfactants or polymers resulting in nanoparticles with diameters up to 10 nm (Gubin et al., 2005).
- Decomposition of metal-containing compounds by ultrasonic treatment is carried out in metal carbonyls and their derivatives being used as metal-containing compounds (Gubin et al., 2005).
- Using strong reducing agents e.g. alkali metal dispersions in ethers or hydrocarbons, alkali metal complexes with organic electro acceptors or high-boiling alcohols, and magnetic metallic nanoparticles can be prepared by the Reduction method (Gubin et al., 2005).
- Sol–gel method, though mostly used to obtain metal oxides, is being used for the synthesis of nanosized metals (Gubin et al., 2005).
- High-energy ball milling is a widely used technique for synthesizing new metastable alloys out from the thermodynamic equilibrium such as amorphous metallic glasses or disordered and

supersaturated solid solutions with achieving a size of below 10 nm (Michalski et al., 2012; Ucar, Ipus, Laughlin, & McHenry, 2013).

Due to sensitivity of nanostructures to milling intensity, temperature and other factors have far-reaching effects on their properties (Saravanan et al., 2008).

4. Metallic nanostructure survey

Table 1 demonstrates that nanostructures are a better choice compared to their bulk counterpart to be utilized in the magnetic refrigeration system. Even though the bulk material has a higher magnetic entropy change, the RCP of the nanostructure is higher than the bulk counterpart. This is very important in the magnetic refrigeration system since increasing the RCP not only increases the amount of refrigeration obtainable from the particular refrigerant and field excursion, but also tends to increase the thermodynamic efficiency of the cycle.

The reduction in magnetization for bulk Pr_2Fe_{17} goes down sharply with temperatures above 280 K, while for the nanostructure Pr_2Fe_{17}, it decreases slowly. At 150 K, the magnetization is 50% greater in the bulk sample but under higher magnetic field, the situation is different, as seen in Figure 4 (Gorria et al., 2008).

Figure 5 shows the improvement in the RCP of a nanostructure compared to its bulk counterpart. Even though the magnetic entropy is higher in the bulk material, the nanostructure Pr_2Fe_{17} has 60% higher δT_{FWHM} compared to the bulk (Gorria et al., 2008).

Three samples of Nd_2Fe_{17} at different particle sizes practically show same MCE properties, but δT_{FWHM} becomes broader with the increase in the milling time and hence reduction in the size. For nanostructure Nd_2Fe_{17} sample, δT_{FWHM} is 72, while for the bulk it is 50 (Alvarez, Gorria, et al., 2010; Alvarez, Sánchez-Marcos, et al., 2010) as shown in Figure 6. A slight improvement of about 5% (Alvarez, Gorria, et al., 2010) is observed in RCP, but in the case of Pr_2Fe_{17}, as seen in Table 1, the improvement in MCE is not that great in the applied magnetic field of 15 kOe.

Curie temperature of Ni nanostructure decreases with the reduction in grain size with a dramatic drop below 10 nm, but its Curie temperature is still above room temperature. The Fe–Ni system, on the other hand, is a good economical and efficient alternative to rare earth-based alternatives. Fe–Ni-based alloys suffer from low magnetic entropy change, thus resulting in a low adiabatic temperature change. However, Fe–Ni-based alloys have low hysteresis and tunable RCP by alloying and breadth of the magnetic transition controlled by impurity- and disorder-derived distributed exchange interactions (Ucar, Craven, Laughlin, & Mchenry, 2014; Ucar et al., 2013).

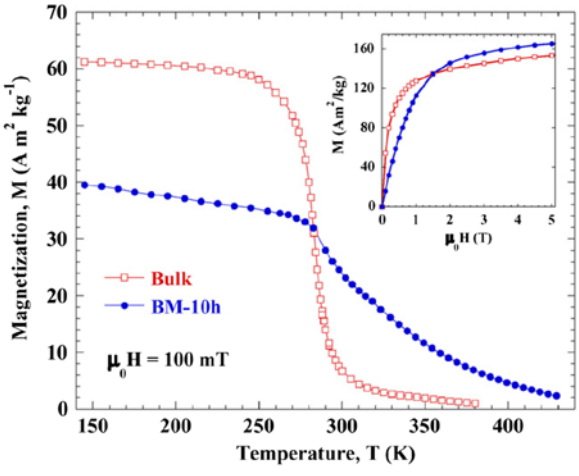

Figure 4. Temperature dependence of the magnetization for both bulk and BM-10h Pr_2Fe_{17} alloys under an applied magnetic field of $\mu_0 H$ = 100 mT.

Note: The inset shows the magnetization vs. applied curves at T = 4 K (Gorria et al., 2008).

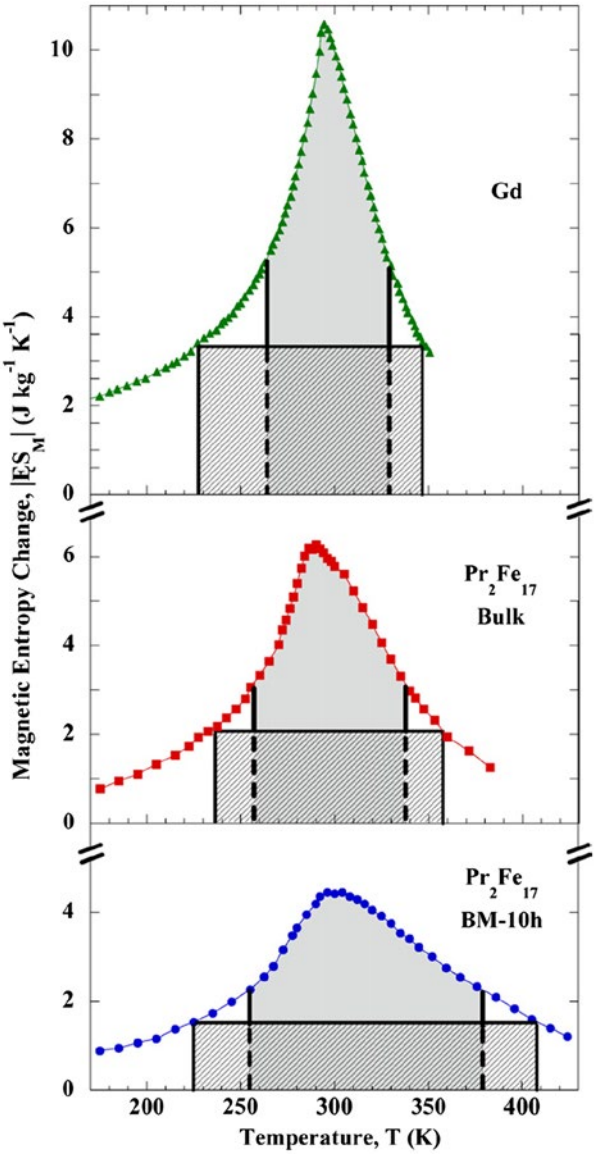

Figure 5. Temperature dependence of calculated $\Delta|S_M|$ and RCP values under an applied magnetic field, $\mu_0 H$ = 5 T, for pure Gd, bulk Pr_2Fe_{17}, and BM-10h Pr_2Fe_{17}.

Note: The RCP values were estimated in two different ways and are shown as the shaded areas and striped rectangles for each material (Gorria et al., 2008).

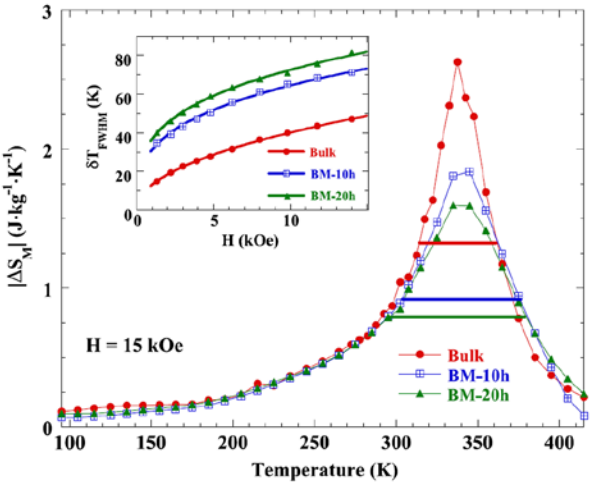

Figure 6. Temperature dependence of $\Delta|S_M|$ under H = 15 kOe for bulk and milled Nd_2Fe_{17} samples.

Notes: The horizontal lines represent δT_{FWHM} for each sample. The inset shows the magnetic field dependence of δT_{FWHM} for all the samples (Alvarez et al., 2010).

As seen in Table 1 (Ucar et al., 2013), even though the compositions of $Fe_{72}Ni_{28}$ and $Fe_{70}Ni_{30}$ are different, the same Curie temperature has been obtained by varying the milling time in preparing the material (50 and 10 h, respectively). Although T_C of $Fe_{70}Ni_{30}$ when milled for 50 h is above room temperature, addition of Mo content can decrease it without decreasing T_C due to broadening of MCE curve because of decrease in magnetic moment and spin-up electron density (Ucar et al., 2014). Alternatively nanoclusters, e.g. Co with size of 2 nm embedded in Ni–Cu matrix, are chosen because of the tenability of their Curie temperature by varying the copper concentration (Michalski et al., 2012). Work by Mukherjee, Sahoo, Skomski, Sellmyer, and Binek (Mukherjee, Sahoo, Skomski, Sellmyer, & Binek, 2009) shows compelling evidence of the benefits of Co/Cr superlattices through modeling and experimental data.

Work by Rong, Li, and Ping Liu (Rong, Li, & Ping Liu, 2007) on Fe_xPt_{100-x} shows the strong effect of controlled composition on its Curie temperature. Moreover, ordered phases with different structures and their formation in different compositional regions are discussed. Ramasamy, Mazumdar, Bennett and Gupta (Ramasamy, Mazumdar, Bennett, & Gupta, 2012) synthesized $CuCr_2Te_4$ by reducing tellurium with sodium borohydride in boiling trioctylamine yielding cube-shaped spinel nanocrystals that have room temperature T_C. Work by Sun et al. (Sun et al., 2012) shows a reduction of 80% thermal and 60% magnetic hysteresis in $MnAs_{0.97}P_{0.03}$ because of 0.68% microstrain presence.

5. Suggestions for new nanostructures

Nanotechnology with its inherent flexibility of tailoring microscopic parameters unlike their bulk counterparts has its advantages (Mukherjee et al., 2009). Table 2 lists metallic and intermetallic bulk materials with magnetic entropy of at least 20 J/kg K and Curie temperature in the range of 260–340 K. As observed in case of Table 1 materials, it is anticipated that synthesizing these materials as nanostructures can achieve more than 40% improvements depending upon the composition of the materials.

6. Summary

MCE data have been gathered for all the metallic nanostructures with Curie temperature between 260 and 340 K in Table 1. When available, nanostructures were compared to their bulk counterparts to understand the effect of nanostructure on MCE properties. In all the cases observed, nanostructures have a profound positive effect on the MCE properties. Metallic nanostructures are important to be considered and further studied for use in magnetic refrigeration technology. In this regard, all metallic bulk materials with magnetic entropy of at least 20 J/kg K have been gathered in Table 2. As observed in the case of Table 1 materials, when bulk materials are synthesized as nanostructures, an improvement of greater that 40% has been reported in their MCE properties. We propose Table 2 materials be synthesized as nanostructures and their MCE properties studied.

Funding
The authors received no direct funding for this research.

Author details
Khurram S. Khattak[1]
E-mail: khattak@gwu.edu
Amir Aslani[1]
E-mail: aaslani@gwu.edu
Chidubem A. Nwokoye[1]
E-mail: lbennett@gwu.edu
Abid Siddique[1]
E-mail: dubem@gwu.edu
Lawrence H. Bennett[1]
E-mail: aabid@gwu.edu
Edward Della Torre[1]
E-mail: edt@gwu.edu
[1] Department of Electrical and Computer Engineering, Institute for Magnetics Research, The George Washington University, Washington, DC 20052, USA.

Citation information
Cite this article as: Magnetocaloric properties of metallic nanostructures, Khurram S. Khattak, Amir Aslani, Chidubem A. Nwokoye, Abid Siddique, Lawrence H. Bennett & Edward Della Torre, *Cogent Engineering* (2015), 2: 1050324.

References

Alvarez, P., Gorria, P., Franco, V., Marcos, J. S., Perez, M. J., Sanchez Llamazares, J. L., ... Blanco, J. A. (2010). Nanocrystalline Nd_2Fe_{17} synthesized by high-energy ball milling: Crystal structure, microstructure and magnetic properties. *Journal of Physics-Condensed Matter, 22*, 216005, 8 pp.

Alvarez, P., Sánchez-Marcos, J., Sanchez Llamazares, J. L., Franco, V., Reiffers, M., Blancoand, J. A., & Gorria, P. (2010, July 6–9). *14th Czech and Slovak Conference on Magnetism*. Košice, Slovakia.

Balli, M., Fruchart, D., Gignoux, D., Dupuis, C., Kedous-Lebouc, A., & Zach, R. (2008). Giant magnetocaloric effect in $Mn_{1-x}(Ti_{0.5}$

$V_{0.5})_x$As: Experiments and calculations. *Journal of Applied Physics, 103*, 103908. http://dx.doi.org/10.1063/1.2917323

Balli, M., Fruchart, D., Gignoux, D., & Zach, R. (2009). The "colossal" magnetocaloric effect in $Mn_{1-x}Fe_x$As: What are we really measuring? *Applied Physics Letters, 95*, 072509. http://dx.doi.org/10.1063/1.3194144

Bedanta, S., & Kleemann, W. (2009). Supermagnetism. *Journal of Physics D-Applied Physics, 42*, 013001. http://dx.doi.org/10.1088/0022-3727/42/1/013001

Bennett, L. H., McMichael, R. D., Swartzendruber, L. J., Hua, S., Lashmore, D. S., Shapiro, A. J., ... Nikitenko, V. I. (1995). Magneto-optical indicator film observation of domain structure in magnetic multilayers. *Applied Physical Letters, 66*, 888–890.

Bennett, L. H., McMichael, R. D., Swartzendruber, L. J., & Shull, R. D. (1992). Monte Carlo and mean field calculations of the magnetocaloric effect of ferromagnetically interacting clusters. *Journal of Magnetism and Magnetic Materials, 104–107*, 1094–1095. http://dx.doi.org/10.1016/0304-8853(92)90504-H

Bennett, L. H., McMichael, R. D., Tang, H. C., & Watson, R. E. (1994). Monte Carlo simulations of the magnetocaloric effect in superferromagnetic clusters having uniaxial magnetic anisotropy. *Journal of Applied Physics, 75*, 5493–5495. http://dx.doi.org/10.1063/1.355667

Bratko, M., Morrison, K., de Campos, A., Gama, S., Cohen, L. F., & Sandeman, K. G. (2012). History dependence of directly observed magnetocaloric effects in (Mn, Fe)As. *Applied Physics Letters, 100*, 252409. http://dx.doi.org/10.1063/1.4729893

Canepa, F., Cirafici, S., Napoletano, M., & Merlo, F. (2002). Magnetocaloric properties of Gd_7Pd_3 and related intermetallic compounds. *IEEE Transactions on Magnetics, 38*, 3249–3251.

Caron, L., Trung, N. T., & Brück, E. (2011). Pressure-tuned magnetocaloric effect in Mn. *Physical Review B, 84*, 020414(R). http://dx.doi.org/10.1103/PhysRevB.84.020414

Chen, X., Sahoo, S., Kleemann, W., Cardoso, S., & Freitas, P. P. (2004). Universal and scaled relaxation of interacting magnetic nanoparticles. *Physical Review B, 70*, 172411. http://dx.doi.org/10.1103/PhysRevB.70.172411

Dagula, W., Tegus, O., Fuquan, B., Zhang, L., Si, P. Z., Zhang, M., ... Buschow, K. H. J. (2005). Magnetic-entropy change in $Mn_{1.1}Fe_{0.9P1-x}Ge_z$ compounds. *IEEE Transactions on Magnetics, 41*, 2778–2780.

Dagula, W., Tegus, O., Li, X. W., Song, L., Brück, E., Cam Thanh, D. T., ... Buschow, K. H. J. (2006). Magnetic properties and magnetic-entropy change of $MnFeP_{0.5}As_{0.5-x}Si_x$(x=0-0.3) compounds. *Journal of Applied Physics, 99*, 08Q105-08Q105-3.

Della Torre, E., Bennett, L. H., & Jin, Y. (2012). An effect of particle size on the behavior of ferromagnetic materials. *Journal of Magnetism and Magnetic Materials, 324*, 2189–2192. http://dx.doi.org/10.1016/j.jmmm.2012.02.010

Dung, N. H., Zhang, L., Ou, Z. Q., Brück, E., & Zhang, J. X. (2011). From first-order magneto-elastic to magneto-structural transition in $(Mn,Fe)_{1.95}P_{0.50}Si_{0.50}$ compounds. *Applied Physics Letters, 99*, 092511. http://dx.doi.org/10.1063/1.3634016

Franco, V., Pirota, K. R., Prida, V. M., Neto, A. Conde, A., Knobel, M., ... Vazquez, M. (2008). Tailoring of magnetocaloric response in nanostructured materials: Role of anisotropy. *Physical Review B, 77*, 104434. http://dx.doi.org/10.1103/PhysRevB.77.104434

Fujieda, S., Fujita, A., & Fukamichi, K. (2007). Enhancement of magnetocaloric effects in $La_{1-z}Pr_z(Fe_{0.88}Si_{0.12})_{13}$ and their hydrides. *Journal of Applied Physics, 102*, 023907. http://dx.doi.org/10.1063/1.2753590

Fujieda, S., Fujita, A., Fukamichi, K., & Suzuki, S. (2011). Influence of homogenization of microstructual composition on hydrogen absorption into $La(Fe_xSi_{1-x})_{13}$ magnetic refrigerants. *IEEE Transactions on Magnetics, 47*, 2459–2462.

Fujita, A., Fujieda, S., Hasegawa, Y., & Fukamichi, K. (2003). Itinerant-electron metamagnetic transition and large magnetocaloric effects in La.FexSi1àx.13 compounds and their hydrides. *Physical Review B, 67*, 104416. http://dx.doi.org/10.1103/PhysRevB.67.104416

Gama, S., Coelho, A. A., de Campos, A., Carvalho, A. M. G., Gandra, F. C. G., von Ranke, P. J., & de Oliveira, N. A. (2004). Pressure-induced colossal magnetocaloric effect in MnAs. *Physical Review Letters, 93*, 237202. http://dx.doi.org/10.1103/PhysRevLett.93.237202

Gorria, P., Sánchez Llamazares, J., Álvarez, P. A., Pérez, M. J., Sánchez Marcos, J. S., & Blanco, J. A. (2008). Relative cooling power enhancement in magneto-caloric nanostructured Pr_2Fe_{17}. *Journal of Physics D: Applied Physics, 41*, 192003, 5 pp. http://dx.doi.org/10.1088/0022-3727/41/19/192003

Gribanov, I. F., Golovchan, A. V., Varyukhin, D. V., Val'kov, V. I., Kamenev, V. I., Sivachenko, A. P., ... Mityuk, V. I. (2009). Magnetic and magnetocaloric properties of the alloys $Mn_{2-x}Fe_xP_{0.5}As_{0.5}$ ($0 \le x \le 0.5$). *Low Temperature Physics, 35*, 786–791. http://dx.doi.org/10.1063/1.3253401

Gschneidner, Jr., K. A., Pecharsky, V. K., Pecharsky, A. O., Zimm, C. B. (1999). Recent developments in magnetic refrigeration. *Materials Science Forum, 315–317*, 69–76. http://dx.doi.org/10.4028/www.scientific.net/MSF.315-317

Gubin, S. P., Koksharov, Y. A, Khomutov, G. B., & Yurkov, Y. G. (2005). Magnetic nanoparticles: Preparation, structure and properties. *Russian Chemical Reviews, 74*, 489–520. http://dx.doi.org/10.1070/RC2005v074n06ABEH000897

Hu, F-x., Shen, B-g., Sun, J-r., Wang, G-j., & Cheng, Z-h. (2002). Very large magnetic entropy change near room temperature in $LaFe_{11.2}Co_{0.7}Si_{1.1}$. *Journal of Applied Physics, 80*, 826–828.

Hu, F. X., Gao, J., Qian, X. L., Ilyn, M., Tishin, A. M., Sun, J. R., & Shen, B. G. (2005). Magnetocaloric effect in itinerant electron metamagnetic systems $La(Fe_{1-x}Co_x)_{11.9}Si_{1.1}$. *Journal of Applied physics, 97*, 10M303.

Kim, Y. K., Wada, H., & Itoh, S. (2007). Shock compaction Of $MnAs_{1-x}Sb_x$ powder using underwater shock wave. *AIP Conference Proceedings, 955*, 1105–1108.

Li, J. Q., Sun, W. A., Jian, Y. X., Zhuang, Y. H., Huang, W. D., & Liang, J. K. (2006). The giant magnetocaloric effect of $Gd_5Si_{1.95}Ge_{2.05}$ enhanced by Sn doping. *Journal of Applied Physics, 100*, 073904. http://dx.doi.org/10.1063/1.2355430

Lima Sharma, A. L., Gama, S., Coelho, A. A., & de Campos, A. (2008). Irreversibility in cooling and heating processes in the magnetocaloric MnAs and alloys. *Applied Physics Letters, 93*, 261910. http://dx.doi.org/10.1063/1.3058712

McMichael, R. D., Shull, R. D., Swartzendruber, L. J., Bennett, L. H., & Watson, R. E. (1992). Magnetocaloric effect in superparamagnets. *Journal of Magnetism and Magnetic Materials, 111*, 29–33. http://dx.doi.org/10.1016/0304-8853(92)91049-Y

Mejía, C., Gomes, A. M., Reis, M. S., & Rocco, D. L. (2011). Fe/Cr substitution in MnAs compound: Increase in the relative cooling power. *Applied Physics Letters, 98*, 102515. http://dx.doi.org/10.1063/1.3560309

Michalski, S., Skomski, R., Li, X-Zh, Le Roy, D., Mukherjee, T., Binek, Ch, & Sellmyer, D. J. (2012). Isothermal entropy changes in nanocomposite $Co:Ni_{67}Cu_{33}$. *Journal of Applied Physics, 111*, 07A930.

Mitsiuk, V. I., Govor, G. A., & Budzyński, M. (2013). Phase transitions and magnetocaloric effect in MnAs, $MnAs_{0.99}P_{0.01}$, and $MnAs_{0.98}P_{0.02}$ single crystals. *Inorganic Materials, 49*, 14–17. http://dx.doi.org/10.1134/S002016851301007X

Mosca, D. H., Vidal, F., & Etgens, V. H. (2008). Strain engineering of the magnetocaloric effect in MnAs epilayers. *Physical*

Review Letters, 101, 125503. http://dx.doi.org/10.1103/PhysRevLett.101.125503

Mukherjee, T., Sahoo, S., Skomski, R., Sellmyer, D. J., & Binek, C. (2009). Magnetocaloric properties of Co/Cr superlattices. *Physical Review B, 79*, 144406. http://dx.doi.org/10.1103/PhysRevB.79.144406

Petracic, O., Chen, X., Bedanta, S., Kleemann, W., Sahoo, S., Cardoso, S., & Freitas, P. P. (2006). Collective states of interacting ferromagnetic nanoparticles. *Journal of Magnetism and Magnetic Materials, 300*, 192–197. http://dx.doi.org/10.1016/j.jmmm.2005.10.061

Ramasamy, K., Mazumdar, D., Bennett, R. D., & Gupta, A. (2012). Syntheses and magnetic properties of Cr_2Te_3 and $CuCr_2Te_4$ nanocrystals. *Chemical Communications, 48*, 5656–5658. http://dx.doi.org/10.1039/c2cc32021e

Recour, Q., Mazet, T., & Malaman, B. (2008). Magnetic and magnetocaloric properties of $Mn_{3-x}Fe_xSn_2$ ($0.1 \le x \le 0.9$). *Journal of Physics D: Applied Physics, 41*, 185002, 5 pp.

Rong, C-B., Li, Y., & Ping Liu, J. (2007). Curie temperatures of annealed FePt nanoparticle systems. *Journal of Applied Physics, 101*, 09K505.

Rongm, C-B., & Ping Liu, J. (2007). Temperature- and magnetic-field-induced phase transitions in Fe-rich FePt alloys. *Applied Physics Letters, 90*, 222504.

Samanta, T., Dubenko, I., Quetz, A., Stadler, S., & Ali, N. (2012). Giant magnetocaloric effects near room temperature in $Mn_{1-x}Cu_xCoGe$. *Applied Physics Letters, 101*, 242405. http://dx.doi.org/10.1063/1.4770379

Samanta, T., Dubenko, I., Quetz, A., Stadler, S., & Ali, N. (2013). Large magnetocaloric effects over a wide temperature range in $MnCo_{1-x}Zn_xGe$. *Journal of Applied Physics, 113*, 17A922.

Sánchez-Valdés, C. F., Ibarra-Gaytán, P. J., Llamazares, J. L. S., Ávalos-Borja, M., Álvarez-Alonso, P., & Blanco, J. A. (2014). Enhanced refrigerant capacity in two-phase nanocrystalline/amorphous $NdPrFe_{17}$ melt-spun ribbons. *Applied Physics Letters, 104*, 212401. http://dx.doi.org/10.1063/1.4879544

Saravanan, P., Gopalan, R., & Chandrasekaran, V. (2008). Synthesis and characterisation of nanomaterials. *Defence Science Journal, 58*, 504–516. http://dx.doi.org/10.14429/dsj

Shir, F., Yanik, L., Bennett, L. H., Della Torre, E., & Shull, R. D. (2003). Room temperature active regenerative magnetic refrigeration: Magnetic nanocomposites. *Journal of Applied Physics, 93*, 8295–8297. http://dx.doi.org/10.1063/1.1556258

Shull, R. D. (1993). Magnetocaloric effect of ferromagnetic particles. *IEEE Transactions on Magnetics, 29*, 2614–2615. http://dx.doi.org/10.1109/20.280849

Shull, R. D., Swartzendruber, L. J., & Bennett, L. H. (1991). The magnetocaloric effect in nanocomposites. In *Proceedings of the Sixth International Cryocoolers Conference* (pp. 231–246). Annapolis, MD.

Skomski, R., Binek, C., Mukherjee, T., Sahoo, S., & Sellmyer, D. J. (2008). Temperature- and field-induced entropy changes in nanomagnets. *Journal of Applied Physics, 103*, 07B329.

Sougrati, M. T., Hermann, R. P, Grandjean, F., Long, G. J, Bruck, E., Tegus, O., ... Buschow, K. H. J. (2008). A structural, magnetic and Mössbauer spectral study of the magnetocaloric $Mn_{1.1}Fe_{0.9}P_{1-x}Ge_x$ compounds. *Journal of Physics-Condensed Matter, 20*, 475206, 9 pp.

Sun, N. K., Cui, W. B., Li, D., Geng, D. Y., Yang, F., & Zhang, Z. D. (2008). Giant room-temperature magnetocaloric effect in $Mn_{1-x}Cr_xAs$. *Applied Physics Letters, 92*, 072504. http://dx.doi.org/10.1063/1.2884524

Sun, N. K., Liu, F., Gao, Y. B., Cai, Z. Q., Du, B. S., Xu, S. N., & Si, P. Z. (2012). Effect of microstrain on the magnetism and magnetocaloric properties of $MnAs_{0.97}P_{0.03}$. *Applied Physics Letters, 100*, 112407. http://dx.doi.org/10.1063/1.3695039

Tocado, L., Palacios, E., & Burriel, R. (2006). Adiabatic measurement of the giant magnetocaloric effect in MnAs. *Journal of Thermal Analysis and Calorimetry, 84*, 213–217. http://dx.doi.org/10.1007/s10973-005-7180-z

Tocado, L., Palacios, E., & Burriel, R. (2009). Entropy determinations and magnetocaloric parameters in systems with first-order transitions: Study of MnAs. *Journal of Applied Physics, 105*, 093918. http://dx.doi.org/10.1063/1.3093880

Trung, N. T., Ou, Z. Q., Gortenmulder, T. J., Tegus, O., Buschow, K. H. J., & Brück, E. (2009). Tunable thermal hysteresis in MnFe(P,Ge) compounds. *Applied Physics Letters, 94*, 102513. http://dx.doi.org/10.1063/1.3095597

Ucar, H., Craven, M., Laughlin, D. E., & Mchenry, M. E. (2014). Effect of Mo addition on structure and magnetocaloric effect in ϒ-FeNi nanocrystals. *Journal of Electronic Materials, 43*, 137–141.

Ucar, H., Ipus, J. J., France, V., Mchenry, M. E., & Laughlin, D. E. (2012). Overview of amorphous and nanocrystalline magnetocaloric materials operating near room temperature. *JOM Journal of the Minerals, Metals and Materials Society, 64*, 782–788.

Ucar, H., Ipus, J. J., Laughlin, D. E., & McHenry, M. E. (2013). Tuning the Curie temperature in -FeNi nanoparticles for magnetocaloric applications by controlling the oxidation kinetics. *Journal of Applied Physics, 113*, 17A918–17A918-3.

Wada, H., Matsuo, S., & Mitsuda, A. (2009). Pressure dependence of magnetic entropy change and magnetic transition in $MnAs_{1-x}Sb_x$. *Physical Review B, 79*, 092407. http://dx.doi.org/10.1103/PhysRevB.79.092407

Yan, A., Müller, K-H., Schultz, L., & Gutfleisch, O. (2006). Magnetic entropy change in melt-spun MnFePGe. *Journal of Applied Physics, 99*, 08K903-08K903-4.

Yue, M., Li, Z. Q., Xu, H., Huang, Q. Z., Liu, X. B., Liu, D. M., & Zhang, J. X. (2010). Effect of annealing on the structure and magnetic properties of $Mn_{1.1}Fe_{0.9}P_{0.8}Ge_{0.2}$ compound. *Journal of Applied Physics, 107*, 09A939.

Yue, M., Liu, D., Huang, Q., Wang, T., Hu, F., Li, J., ... Zhang, J. (2013). Structure evolution and entropy change of temperature and magnetic field induced magneto-structural transition in $Mn_{1.1}Fe_{0.9}P_{0.76}Ge_{0.24}$. *Journal of Applied Physics, 113*, 043925. http://dx.doi.org/10.1063/1.4788803

Zeng, H., Kuang, C., Zhang, J., & Yue, M. (2012). Magnetocaloric effect in bulk nanocrystalline Gd metals by spark plasma sintering. *Nanoscience Methods, 1*, 16–24. http://dx.doi.org/10.1080/17458080.2010.515251

Zhang, H., Long, Y., Niu, E., Shao, X. P., Shen, J., Hu, F. X., ... Shen, B. G. (2013). Influence of particle size on the hydrogenation in $La(Fe, Si)_{13}$ compounds. *Journal of Applied Physics, 113*, 17A911.

Zhang, H., Shen, B. G., Xu, Z. Y., Zheng, X. Q., Shen, J., Hu, F. X., ... Long, Y. (2012). Reduction of hysteresis loss and large magnetocaloric effect in the C- and H-doped $La(Fe, Si)_{13}$ compounds around room temperature. *Journal of Applied Physics, 111*, 07A909.

Zhao, J-l., Shen, J., Hu, F-x., Li, Y-x., Sun, J-r., & Shen, B-g. (2010). Reduction of magnetic hysteresis loss in $La_{0.5}Pr_{0.5}Fe_{11.4}Si_{1.6}H_x$ hydrides with large magnetocaloric effects. *Journal of Applied Physics, 107*, 113911. http://dx.doi.org/10.1063/1.3374635

Cogent Engineering **(ISSN: 2331-1916) is published by Cogent OA, part of Taylor & Francis Group.**